BJPS

Brazilian Journal of
Pharmaceutical Sciences

http://dx.doi.org/10.1590/s2175-97902023e21159

Article

Study of antidiabetic activity of two novel Schiff base derived dibromo and dichloro substituted compounds in streptozotocin-nicotinamide-induced diabetic rats: pilot study

Kamelia Saremi[1]*, Sima Kianpour Rad[2], Zohreh Shahnavaz[3], Nazia Binti Abdul Majid[1]

[1]Institute of Biological Science, Faculty of Science, University of Malaya, Kuala Lumpur, Malaysia, [2]Discipline of Surgery, Adelaide Medical School, The University of Adelaide, Adelaide, SA, Australia The Basil Hetzel Institute for Translational Health Research, The Queen Elizabeth Hospital, Adelaide, SA, Australia, [3]School of Materials Science and Engineering, Jiangsu University, Zhenjiang 212013, Jiangsu, PR China

Schiff bases are aldehyde-or ketone-like chemical compounds in which an imine or azomethine group replaces the carbonyl group. Such compounds show various beneficial biological activities, such as anti-inflammation and antioxidants. The present study addresses comprehensive evaluation of antidiabetic effect of two novel dibromides and dichlorides substituted Schiff bases substituted Schiff bases (2,2'-[1,2-cyclohexanediylbis (nitriloethylidyne)]bis[4-chlorophenol] (CNCP) and 2, 2'-[1,2-cyclohexanediylbis(nitriloethylidyne)]bis[4-bromophenol] (CNBP) with two different doses, high (LD) and low (LD) in streptozotocin and nicotinamide induced diabetic rats. The rats were separated into normal, untreated, treated and reference groups. Except for the normal group, diabetes traits were induced in the rest animals. Insulin level was measured, and the effect of the compounds on biochemical parameters of liver function and lipid profile were evaluated. High glucose and decreased insulin level are observed in the groups. The histological evaluation confirms that the hepatic architecture in the treated animals with a low dose of CNCP is quite similar to that of the normal hepatic structure and characterized by normal central vein, hepatocytes without any fatty alterations and mild red blood cell infiltration. CNCP (LD) and CNBP (HD) are more successful in enhancing cell survival in the diabetic rat's liver and can be responsible for causing much healthier structure and notable morphology improvement.

Keywords: CNCP. CNBP. Schiff base. Dichloride substitution. Dibromid substitution. Anti-diabetic effect.

INTRODUCTION

When β cells of pancreatic islets, which normally produce insulin, are unable to produce and/or release adequate insulin to overcome peripheral insulin resistance, TD2M accurse. Decreasing insulin secretion and its sensitivity (insulin resistance) have significant accountability for the disease pathogenesis, although, the trend for insulin resistance may not always be detected (Zhao *et al*., 2017). Experimental diabetes mellitus can be vastly induced in animals by several different methods. Noshahr *et al*., 2020 induced diabetes type two in animals by administering an appropriate dose of nicotinamide (NIC) before STZ administration. In this method, NIC wields an incomplete form of protection against the detrimental cytotoxic effects of STZ (Noshahr *et al*., 2020). NIC, a form of vitamin B3, is water-soluble and known as a poly-ADP-ribose synthesis inhibitor, showing a protective effect on β-cells. Such protection against STZ-induced destruction of β-cells can be railed by two substantial mechanisms, such as inhibiting PARP-1 and

***Correspondence:** K. Saremi. Institute of Biological Science. Faculty of Science. University of Malaya. 50603, Kuala Lumpur, Malaysia. Orcid: https://orcid.org/0000-0002-1893-6830

elevating the concentration of NAD+ (Lenzen, 2017). This in turn can enrich energy status and demonstrates protective antioxidant effects. The process then leads to metabolic improvement via inhibition of mass apoptosis of β-cell by partially reversing the inhibition of insulin secretions to arrest or halt the complete aggravation of β-cells damage following the dispensation of STZ dose (Shima, Zhu, Kuwajima, 1998).

T2DM is associated with various liver disorders, including fatty liver disease, elevated liver enzymes cirrhosis, hepatocellular carcinoma, and acute liver failure. Measurements of the activity of serum aspartate transaminase (AST), alanine transaminase (ALT) and alkaline phosphatase (ALP) are considered the most sensitive tests are contributing to the diagnosis of organs damage, including kidney and liver. An increase in the serum AST, ALT, or ALP activity of STZ-induced diabetic mice is an indicator of liver and kidney destruction, probably due to lipid peroxidation leading to free radical production (Kim, 2014).

Free radical production and inflammation enhance oxidative stress and play a basic role in the pathogenesis and progression of diabetic disease (Kakkar *et al.*, 1995). In such conditions, antioxidants inhibit oxidation of biomolecules by shielding effects and accordingly boost the immune system against detrimental effects of ROS (Lobo *et al.*, 2010).

Antioxidants are overall hydrogen or electron donors to the reactive site for neutralizing free radicals (Kumar, Padmini, Ponnuvel, 2017). The radical scavenging activity of organic compounds is assessed using 2, 2-diphenyl-1-picrylhydrazyl (DPPH), hydrogen peroxide, superoxide anion radical, and ABTS+. It is reported that a broad range of organic molecules acts as potent antioxidants; therefore, it is important to understand the mechanisms of action and efficiency of such antioxidants. Large numbers of natural and synthetic antioxidants are identified, and their antioxidant capacity has been assessed by different methods, such as the DPPH radicals scavenging assay (Kumar, Padmini, Ponnuvel, 2017).

Numerous strategies and medications have been found in order to prevent diabetes; however, the management of this disorder has remained profoundly unsuccessful. Among available treatments, hypoglycemic agents, phenformin, troglitazone, rosiglitazone and repaglinide can control hyperglycemia, but some undesirable adverse-effects are reported with such drugs (Gupta, 2010).

Schiff-base compounds are of those candidates, which have drawn researchers' attention in recent years due to their synthetic flexibility, relative easiness of preparation and outstanding biological activities (Ndagi, Mhlongo, Soliman, 2017). Schiff bases are an important class of compounds containing azomethine or imine (−C═N−) moiety. This pharmacophore is utilized to design and develop various medicinally important molecules and emerging drugs. In many reports, a high pharmaceutical value of the azomethine group is associated with the presence of an electron lone pair in the nitrogen atom (Anitha *et al.*, 2013; Sirajuddin *et al.*, 2012; Sahiba *et al.*, 2020).

Various Schiff base-containing derivatives have been reported as potential antidiabetic agents, including, pioglitazone (Afzal *et al.*, 2021), metformin hydrochloride and (ortho) para-nitrobenzaldehyde (Al-Qadsy *et al.*, 2020), Salicylaldehyde and beta-alanine (Vančo *et al.*, 2008), chromium (III) complexes of metformin Schiff -bases (Mahmoud *et al.*, 2016) and Vanadyl Schiff-base Complexes (Torabi, Mohammadi, Shirvani, 2018). In addition, it is noted that bromine (Lin, Liu, 2012; Niizato, Shiotani, Shoji, 2002) and chlorine (EL-Hashash, Kadhim, Rizk, 2015; Mahmoud *et al.*, 2016; Shukla *et al.*, 2019) substituted complex of chemical drugs can exhibit excellent effects against diabetes by lowering the glucose level in the body.

In the current pilot work, anti-diabetic activity CNCP and CNBP, two dibromide and dichloride substitutes of the same Schiff base, were analyzed in the rodent model by evaluating the liver and kidney enzymes activities and blood insulin level. The two compounds showed potent antioxidant and antidiabetic potentials.

MATERIAL AND METHODS

Material

All the necessary chemicals for the syntheses were purchased from Merck and Sigma-Aldrich chemical companies. SD rats were obtained from the Animal Experimental Unit (AEU), Faculty of Medicine,

University of Malaya. Paraffin tissue processing equipment, ketamine and xylazine for anaesthetizing the animals and tween 20 were purchased from Sigma-Aldrich, Germany. Omeprazole was obtained from TROGE Medical GMBH, Germany. Sucrose, magnesium chloride and alcian blue, MTT reagent, thiazolyl blue and tetrazolium bromide were all purchased from USB Affymetrix.

Synthesis and characterization of CNCP

The Schiff bases derivatives, entitled; 2, 2'-[-1,2-cyclohexanediylbis(nitriloethylidyne)]bis(4-chlorophenol) (CNCP) and 2, 2′-[1, 2-cyclohexanediylbis(nitriloethylidyne)]bis(4-bromophenol) (CNBP) were prepared through the following protocol (Yaul *et al.*, 2013). First, a solution of trans-1,2-diaminocyclohexane (3.0 g, 26.27 mmol for CNCP and 2.5 g, 21.9 mmol for CNBP) in methanol (80 ml for CNCP and 70 ml for CNBP) was reacted with 5-chloro-2-hydroxyacetophenone (8.96 g, 52.54 mmol) under reflux condition for 6 hours. After cooling to ambient temperature, two separate yellowish solid crystals. Then, the two compounds were formed, filtered, washed with methanol, and dried over phosphorus pentoxide. Finally, they were recrystallized from ethanol to yield CNCP (8.82 g, 80%) m.p. 228–230 °C.I and CNBP (8.45 g, 76%), m.p. 220–222 °C (Figure 1).

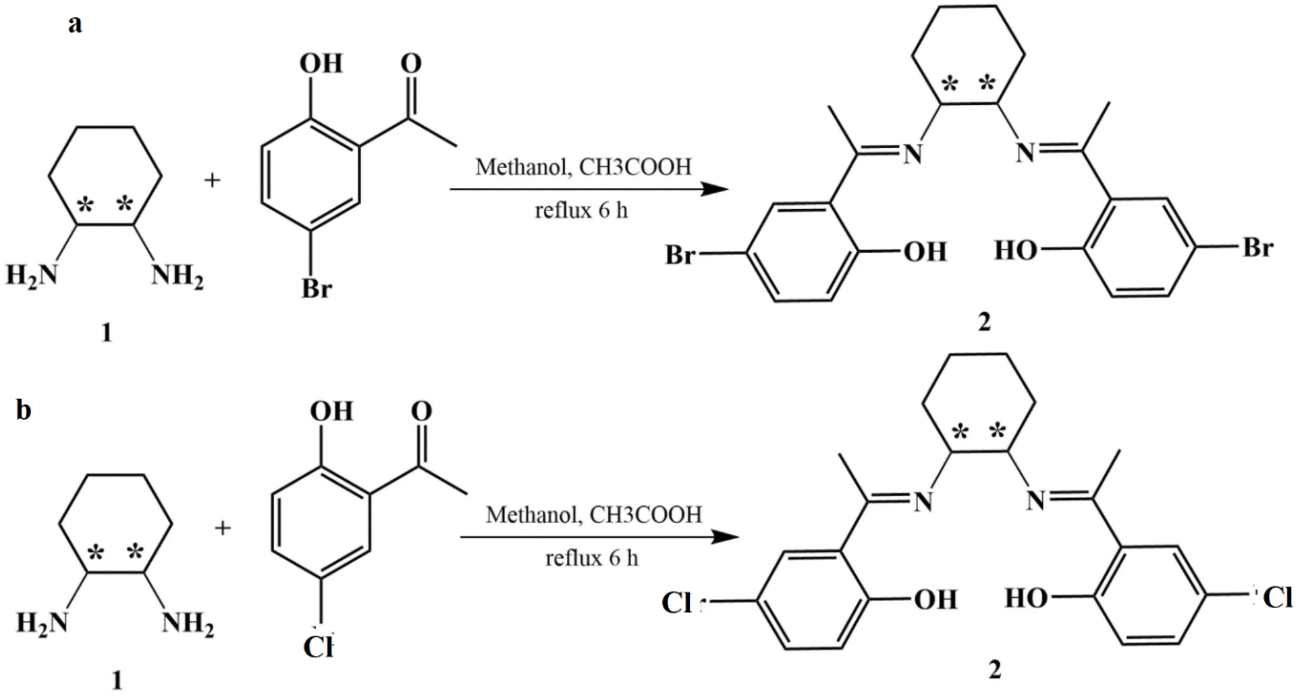

FIGURE 1 - Synthesis of CNBP (a) and CNCP(b).

Purification and structural elucidation of compounds by NMR

The structures and purity of both compounds were confirmed by spectroscopic methods, 1H and 13C NMR.

1H NMR of the chemical structure of 2, 2-[1,2-cyclohexanediylbis (nitriloethylidyne)] bis(4-chlorophenol) (CNCP) shows two doublet signals of four aromatic protons at about δ 7.34 and δ 6.79 ppm as well as a double doublet signal of two aromatic protons at about 7.16 ppm. The protons for two groups of CH-N show double triplet to multiple signals at about 3.85 ppm. The protons of the CH3 groups appear as a singlet signal

at 2.25 ppm. While the rest protons of the cyclohexane ring show triplet to multiple signals at about 1.9, 1.67 and 1.48 ppm, respectively.

13C NMR spectra show the signals of the two C=N at about δ 170.17 ppm. The spectra also show the presence of the two carbons signals attached to hydroxyl groups at 162.28 ppm. The tertiary carbons of the aromatic rings appear at about 132.40, 127.90 and 120.09. Whereas, quaternary carbon, CAr-Cl and CAr-CN, at 121.84 and 119.9 ppm respectively. The CH-N carbons were found δ 63.27. The positions of cyclohexane carbons methylene at δ 32.32 and 24.19 and methyl carbons were located around δ 14.55 ppm. 13C NMR is used to assign the carbon skeleton, applying the PENDANT (Polarization Enhancement Nurtured during Attached Nucleus Testing) experiment to distinguish carbons attached to varying numbers of H. In PENDANT spectra, carbons attached to odd numbers of protons (methyl, CH3; methine, CH) appear as negative signals, whereas those attached to even numbers of protons (methylene, CH2; quaternary, C) appear as positive signals.

1H NMR of the chemical structure of 2,2-[1,2-cyclohexanediylbis (nitriloethylidyne)]bis(4-bromophenol) (CNBP) shows two doublet signals of four aromatic protons at about δ 7.34 and δ 6.79 ppm as well as a double doublet signal of two aromatic protons at about 7.16 ppm. The protons for two groups of CH-N show double triplet to multiple signals at about 3.85 ppm. The protons of the CH3 groups appear as singlet signal at 2.25 ppm. While the rest protons of cyclohexane ring show triplet to multiple signals at about 1.9, 1.67 and 1.48 ppm respectively

13C NMR spectra show the signals of the two C=N at about δ 170.17 ppm. The spectra also show the presence of the two carbons signals attached to hydroxyl groups at 162.83 ppm. The tertiary carbons of the aromatic rings appear at about 135.24, 130.87 and 120.82. Whereas quaternary carbon, CAr-Br and CAr-CN, at 120.62 and 108.79 ppm, respectively. The CH-N carbons were found δ 63.21. The positions of cyclohexane carbons methylene at δ 32.33 and 24.19 and methyl carbons were located around δ 14.57 ppm.

The compounds are characterized by the following data:

CNCP (8.82 g, 80%)**,** m.p. 228–230°C. IR [KBr]: 3500 cm^{-1} (OH), 3010 cm^{-1} ($CH_{aromatic}$), 2937, 2861 cm^{-1} ($CH_{aliphatic}$), 1609 cm^{-1} (C=N), 1565 cm^{-1}(C=C), 1256 cm^{-1} (C-N). ^{1}H NMR (400 MHz, $CDCl_3$): *δ* 7.34 (d, 2H, ^{3}J = 2.6 Hz, 2× Ar-H), 7.16 (dd, 2H, ^{3}J = 8.8 Hz, 2× Ar-H), 6.79 (d, 2H, ^{3}J = 8.8 Hz, 2× Ar-H), 3.85 (dt~m_c, 2H, 2× CH-N), 2.25 (s, 6H, 2× CH_3), 1.9 (t, 4H, ^{3}J = 9.5 Hz, 2× CH_2-CH), 1.67 (p~m_c, 2H, CH_2), 1.48 (p~m_c, 2H, CH_2).^{13}C NMR (100 MHz, $CDCl_3$): *δ* 170.17 2× (C=N), 162.28 2× (Ar-OH), 132.40, 127.90 2× (CH_{Ar}) 121.84 2× (Ar-Cl), 120.09 2× (CH_{Ar}), 119.9 2× (C_{Ar}-CN), 63.27 2× (CH-N), 32.32, 24.19 2× (CH_2CH_2), 14.55 2× (CH_3).

CNBP (8.45 g, 76%), m.p. 220–222 °C. IR [KBr]: 3500 cm− 1 (OH), 3020 cm− 1 ($CH_{aromatic}$), 2940, 2860 cm− 1 ($CH_{aliphatic}$), 1605 cm^{-1} (C=N), 1560 cm^{-1}(C=C), 1256 cm^{-1}(C-N); 1H NMR (400 MHz, CDCl3): δ 7.60/(7.48) (d, 2H, 3J = 2.4 Hz, 2x Ar-H), 7.30/(7.29) (dd, 2H, ^{3}J = 8.9 Hz, 2x Ar-H), 6.77/(6.75) (d, 2H, ^{3}J = 8.9 Hz, 2x Ar-H), 4.60/(3.85) (mc, 2H, 2x CH-N), 2.32/(2.25) (s, 6H, 2x CH_3), 1.9 (t~mc, 4H, 2x CH_2-CH), 1.79–1.57 (mc, 2H, CH_2), 1.48 (p~mc, 2H, CH_2).13C NMR (100 MHz, CDCl3): δ 170.16 (169.95) 2x (C=N), (163.01) 162.83 2x (Ar-OH), 135.24 (135.16), 130.87 (130.70) 2x (CHAr) 120.82 (120.78) 2x (CAr-CN) 120.62 (120.51) 2x (CH_{Ar}), 108.79 (108.57) 2x (Ar-Br), 63.21 (59.61) 2x (CH-N), 32.33 (29.81), 24.19 (22.29) 2x (CH_2CH_2), 14.57 (14.52) 2x (CH_3).

Based on the above information, elemental analysis (%C, %H, %O, etc.) of our compounds, in comparison with the net weight of the compounds, show that CNCP and CNBP were 80% and 76% pure, respectively.

Antioxidant study

The scavenging activity of 2,2-diphenyl-1-picrylhydrazyl (DPPH) (Merck, Darmstadt, Germany) radicals by both compounds was tested, and their cytotoxicity effects were completely evaluated. The results are available from our previous studies (Saremi *et al.*, 2019; 2020).

In vitro assays

Acute toxicity and experimental design

The results of acute toxicity of CNBP and CNCP were already published (Saremi *et al*., 2019; 2020).

In vivo assays

Animal procedure

Forty-two healthy male SD rats (6–8 weeks old, 200–250 g) were purchased from the Animal Experimental Unit, Faculty of Medicine of the University of Malaya. The mice were then housed in plastic cages in a department laboratory with a standardized environment with a temperate of 23 ± 2 °C and a routine dark cycle (12 h light/ 12 h). The animals were left to have water, *libitum* and standard chow pellets while they also were acclimatized to the condition, which caused them to be observed 1 day before the experiments. The experimental processes, including the protocols in this study, were approved by the Ethics Committee of the Research Centre and in accordance with the recommendations of the University of Malaya; Council on Animal Care Guidelines for the proper care and use of laboratory animals (Ethic no. 2015-09-11/BMS/R/MAA).

Type 2 diabetes induction

Injection of STZ was used to induce diabetes in the animals based on the protocol described and tested by with some minor modifications (Masiello *et al*., 1998). STZ was freshly dissolved in 0.05 M citrate buffer (pH 4.5) and was injected intraperitoneally (ip) into the overnight-fasted healthy male rats with the dose of 60 mg/kg after 15 min of ip administration of 210 mg/kg nicotinamide (NA). Diabetes induction in the rats was confirmed by finding out if there was elevated glucose level, measured using a glucometer from one drop of blood taken from the tail vein of each animal post 48 hours of the injection. The fasting rats with a blood glucose reading of > 200 mg/dl were speculated to be diabetic animals (Bedia *et al*., 2006). The compounds to be examined were administered orally to the animals for 45 days daily. The blood glucose level and body weight were measured weekly, and food and water intake were recorded regularly.

Grouping and treatments

The rats were assembled into seven groups (each group had six animals) and orally gavaged with relative drugs for 45 days, viz:

G1: Healthy control rats (vehicle, fed with 10% tween 20)
G2: Untreated control rats (fed with 10% tween 20)
G3: Untreated control reference rats (fed with glibenclamide (600 µg/kg)
G4: Diabetic rats 1 (treated with CNCP (10 mg/kg, LD))
G5: Diabetic rats 2 (treated with CNCP (20 mg/kg, HD))
G6: Diabetic rats 3 (treated with CNBP (10 mg/kg, LD))
G7: Diabetic rats 4 (treated with CNBP (20 mg/kg, HD))

Biochemistry parameters examination

After completely clotted, the blood samples were separated by centrifugation at 2500 rpm for 15 min. Then, the blood serum was assessed spectrophotometrically using an automated, standardized technique based on the procedure described in the laboratory manual of the Central Diagnostic Laboratory, University of Malaya Medical Centre, for evaluating liver function and lipid profile.

Fasting blood glucose measurement

At days 1, 7, 15 and 45, fasting blood glucose concentrations were determined using an Accu-check Advantage II Glucometer and compatible blood glucose test strips. The percentage of variation of glycaemia was calculated based on the formula below, where x was considered separately for days 7, 15 or 45 (Küçükgüzel *et al*., 2005).

$$\%\, Variation\ of\ glycaemia\ =\ \frac{Day\ x - Day\ 1}{Day\ 1} \times 100$$

Body weight changes measurement

A digital weight scale measured the rats' body weight (grams) before and after the experiments. The body weight changes were calculated via the following formula;

$$\frac{Body\ weight\ (Day\ 45)\ -\ Body\ weight\ (Day\ 1)}{Body\ weight\ on\ Day\ 1} \times 100$$

Measurement of insulin

The assay to measure insulin level was based on the sandwiched ELISA principle using a commercially available ELISA assay kit (Rat Insulin ELISA kit). Different serials concentrations (0.2, 0.5, 1, 2, 5, 10 ng/ml) of rat insulin standards, control and samples at an equal volume of 10 µl were added into each well. First, an 80 µl detecting antibody was added to each well, and then the plate was incubated at an ambient temperature for 2 hours on a microtiter plate shaker with a speed of 400-500 rpm. After incubation, the solution was aspirated from the wells, and any residuals were removed by gently tapping and then rinsed with the prepared washing buffer. Next, 100 µl of enzyme solution was added to every well, followed by a half-hour incubation period at room temperature on a microtiter plate shaker with moderate shaking. Next, a buffer was used to wash the coated wells, and then a 100 µl of substrate solution was added to each well, followed by shaking on a microtiter plate shaker for 15 min. After adding 100 µl stop solutions, the blue colour observed in the standard wells changed to yellow at this stage. The absorbance was read at 450 nm within 5 min.

Histological study of diabetic tissues

Routine Hematoxylin and Eosin staining

The kidney, liver and pancreas tissue samples were fixed in 10% buffered formalin, then administered in a paraffin tissue-processing device, followed by being embedded in paraffin blocks. The pieces (5µm) were stained by Hematoxylin and Eosin (H&E), considered standard staining to assess tissue architecture. The stained samples were used for microscopic analysis (Rollas, Gulerman, Erdeniz, 2002).

Statistical analysis

All data are accessible as mean ± SEM. Differences among the experimental groups were determined by one-way ANOVA followed by Tukey's post-hoc test for multiple comparisons using SPSS version 24. Values of $p< 0.05$ were considered significant.

RESULTS

Antioxidant activity and cytotoxicity effects

The results of cytotoxicity evaluations of both CNCP and CNBP were published in our previous articles (Saremi *et al.*, 2019, 2020). It was shown that the both compounds could improve proliferation of dermal fibroblast cells and had no cytotoxicity effects. The maximum concentrations for drastic enhancement of the cell proliferation were detected at 6.2 to 12.5 µg/ml for CNCP. Also, for CNBP, the threshold concentrations for significant increase of cell proliferation was detected as 12.5 to 25 µg/ml. Also, in the articles, it was showed that CNBP and CNCP with IC_{50} of 30.86 and 29.00 µg/ml respectively, could showed acceptable DPPH scavenging activities in comparison with ascorbic acid (standard) with an IC_{50} of 8.84 µg/ml. It was demonstrated that CNCP was more active to scavenge the DPPH radicals than CNBP.

Acute toxicity study

The effects of acute toxicity study of CNBP and CNCP were already published. (Saremi *et al.*, 2019, 2020). In the treated groups, no mortality and definite sign of toxicity in the CNCP and CNBP- treated animals was detected when comparing with the control group (vehicle). The histological study confirmed no evidence of acute toxicity of the both compounds on liver and kidney in all the studied groups.

Biochemistry analysis

As listed in Table I, total protein and albumin levels in the untreated control group were significantly declined when compared to the healthy control group. Both CNCP (low dose, LD) and CNBP (high dose, HD) increased total protein amounts as well as albumin levels. CNCP (LD) showed highest increase in the total protein amount and in the albumin levels versus the untreated controlled animals. Table I lists the values which are associated with the effect of both CNCP and CNBP (LD and HD) on AST, ALT, and ALP activity in the serum of the normal, treated, and untreated diabetic rats. As observed, the enzymes activities in the serum of untreated diabetic rats were significantly increased; while AST, ALT, and ALP activity in the serum of CNCP (LD) and CNBP (HD)-treated animals showed noticeable decrease in 6 weeks of post treatment therapy.

Effect of CNCP and CNBP at both low doses (LD=10 mg/kg) and high dose (HD=20 mg/k) as well as glibenclamide, total cholesterol, and high density lipoprotein (HDL) and low density lipoprotein (LDL) cholesterol level in the treated, untreated diabetic normal, and also control rats is listed in Table I. The serum triglyceride, total cholesterol, and LDL cholesterol levels in the untreated diabetic rats were remarkably increased when compared to those of the healthy control rats; however, HDL cholesterol level in the untreated diabetic rats showed totally reversed effects. The serum triglyceride, total cholesterol, and LDL cholesterol levels were significantly reduced by treatment with either glibenclamide or CNCP (LD) and CNBP (HD), while, HDL cholesterol level were increased compared to that of the untreated diabetic rats after 6-week treatment period. Evidently, it is postulated that continuous treatment with the both compounds could help decrease the lipid parameters in diabetic rats.

TABLE I - Effect of CNCP, CNBP, and glibenclamide on biochemical parameters in liver function and lipid profile of normal and STZ-NA-induced diabetic rats after 45 days of treatment

Assay	Healthy Control	Diabetic Animal	Glibenclamide	CNCP (LD)	CNCP (HD)	CNBP (LD)	CNBP (HD)
Total protein (g/dL)	8.20 ± 2.66	5.20 ± 1.46	7.10 ± 2.07*	6.60 ± 2.29*	6.20 ± 2.02*	5.90 ± 1.00*	6.50 ± 1.20*
Albumin (g/dL)	5.40 ± 1.76	3.20 ± 2.56	4.80 ± 1.25*	4.60 ± 2.70*	3.76 ± 1.90*	4.37 ± 0.33*	4.67 ± 0.56*
Liver function							
ALP (IU/L)	69.60 ± 2.99	110.40 ± 2.10	66.60 ± 2.86*	72.20 ± 2.13*	78.80 ± 2.91*	79.33 ± 2.18*	73.67 ± 2.06*
AST (IU/L)	55.00 ± 2.23	92.60 ± 2.72	61.00 ± 2.95*	67.60 ± 2.34*	79.60 ± 2.86*	82.33 ± 2.09*	68.67 ± 2.05*
ALT (IU/L)	46.80 ± 2.68	77.40 ± 2.05	52.80 ± 2.34*	60.40 ± 2.82*	67.80 ± 2.90*	66.00 ± 2.24*	62.00 ± 2.16*
Lipid profile							
Triglyceride (mmol/L)	1.56± 0.10	2.65 ± 0.15	1.59± 0.07*	1.62 ± 0.17*	1.96± 0.31*	1.84± 0.15*	1.64± 0.24*
Total cholesterol (mmol/L)	2.36± 0.17	3.23 ± 0.15	2.57± 0.17*	2.48 ± 0.38*	2.64± 0.12*	2.60± 0.10*	2.43± 0.48*
HDL Cholesterol (mmol/L)	1.88± 0.12	1.00 ± 0.20	1.73± 0.03*	1.52 ± 0.05*	1.42± 0.15*	1.46± 0.6*	1.51± 0.9*
LDL Cholesterol (mmol/L)	0.23± 0.11	0.61± 0.10	0.26± 0.13*	0.29 ± 0.34*	0.32± 0.17*	0.31± 0.15*	0.29± 0.27*

All values are presented as mean ± standard error mean, compared to untreated control (n = 6). $^{*}P<0.05$ is considered as significant. ALP = alkaline phosphatase; ALT = alanine aminotransaminase; AST = aspartate aminotransaminase.

IU/L= international unit per liter

Physiological parameters of animals

In Figure 2, the level of blood glucose in the treated group is assessed against those in the untreated control group. The untreated control group showed higher glucose levels in comparison to the healthy control group. Regarding to percentage decrease of blood glucose level following each treatment at different doses (day 45), (CNCP (LD), CNBP (HD)) and glibenclamide decreased glucose level (Figure 2). It is noticed that blood glucose levels in the diabetic rats was significantly decreased after treating with CNCP (LD), CNBP (HD) as well as glibenclamide from day 21 to 45. However, the doses of the both compounds produced significant reduction in the blood glucose level post day 21 and showed highest lessening rate at day 45 in comparison with the untreated control group. The highest percentage of variation of glycaemia is seen at day 45, which belonged to CNCP (LD, -31.28 ± 12.80) (Table II). Therefore, the findings confirmed that both compounds (CNCP and CNBP) decreased blood glucose levels in the diabetic rats.

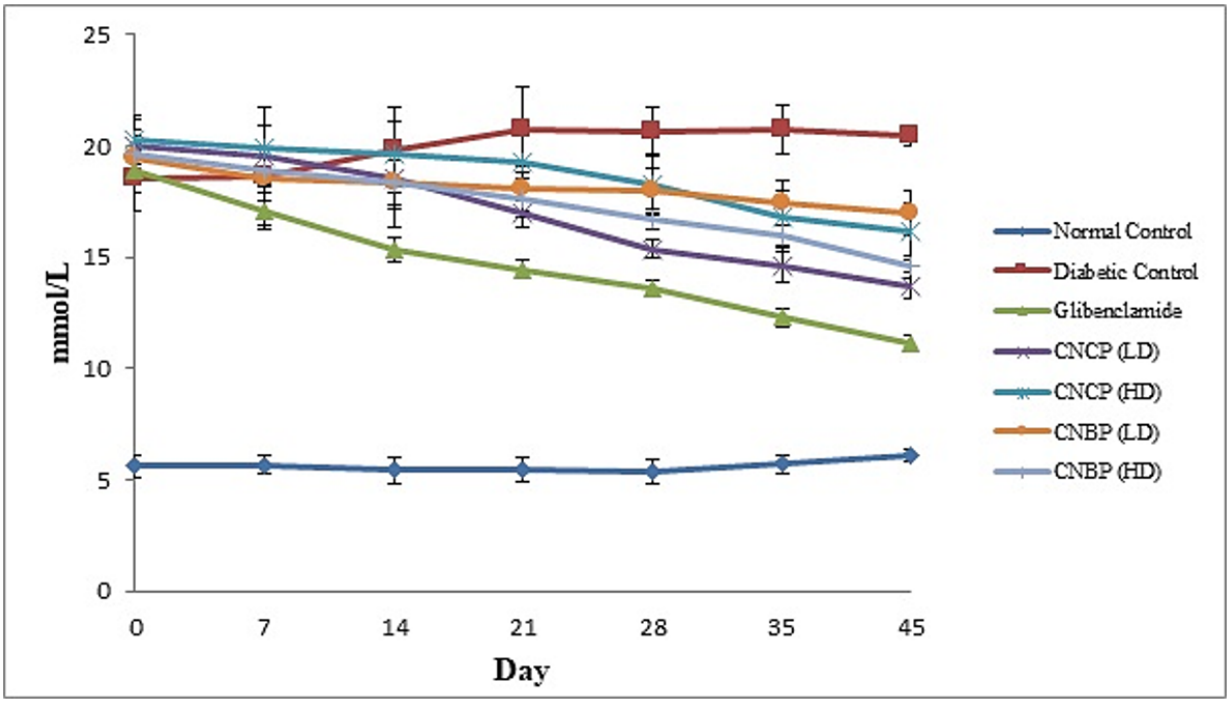

FIGURE 2 - Fasting blood glucose levels in STZ-NA-induced diabetic and control rats for 45 days. All values are recorded as Mean ± SEM (n=6).

TABLE II - Percentage of variation of glycaemia ± SEM. (mg/dl)

Test samples	Dose	Day 0	Day 7	Day 14	Day 21	Day 28	Day 35	Day 45
Healthy Control	_	0 ± 0.0	0.89 ± 2.06	-3.38 ± 4.38	-3.70 ± 6.20	-4.63 ± 7.44	1.42 ± 9.24	8.54 ± 11.27
Untreated control	_	0 ± 0.0	0.43 ± 2.00	6.95 ± 4.76	11.80 ± 6.81	11.31 ± 7.95	11.58 ± 9.22	10.34 ± 10.26
Glibenclamide	600 (µg/kg)	0 ± 0.0	-9.58 ± 2.49	-18.74 ± 4.88	-23.50 ± 6.63	-27.79 ± 8.26	-34.94 ± 10.12	-41.13 ± 12.14
CNCP (LD)	10 (mg/kg)	0 ± 0.0	-2.00 ± 2.06	-7.31 ± 4.14	-14.96 ± 6.45	-23.07 ± 8.67	-26.73 ± 10.64	-31.28 ± 12.80
CNCP (HD)	20 (mg/kg)	0 ± 0.0	-1.58 ± 2.34	-3.11 ± 4.25	-5.08 ± 6.02	-9.87 ± 7.86	-17.32 ± 10.23	-20.37 ± 12.63

TABLE II - Percentage of variation of glycaemia ± SEM. (mg/dl)

Test samples	Dose	Day 0	Day 7	Day 14	Day 21	Day 28	Day 35	Day 45
CNBP (LD)	10 (mg/kg)	0 ± 0.0	-4.73 ± 2.39	-5.65 ± 4.20	-6.99 ± 5.96	-7.55 ±7.66	-10.38 ± 9.52	-12.90 ± 12.5
CNBP (HD)	20 (mg/kg)	0 ± 0.0	-3.77 ± 1.79	-6.72 ± 3.43	-10.13 ± 5.02	-14.96 ± 6.82	-18.63 ± 8.45	-25.90 ± 10.97

All values are presented as mean ± SEM, compared to untreated control groups (n = 6). $p < 0.05$ is considered as significant. The negative value (−) demonstrated a decrease in glycaemia.

Body weight changes

The diabetic rats treated with different concentrations of low dose of CNCP (LD, 10 mg/kg) and high dose of CNBP (HD, 20 mg/kg), respectively caused an increase in body weight when the weights were compared with the untreated diabetic rats. At day 14, no significant difference was found in body weight between the rats treated with both concentrations of CNCP and CNBP. However, at day 28, the rats treated with CNCP (LD) and CNBP (HD) showed an increase in weight gain, compared to diabetic rats. Furthermore, at day 45, those rats receiving low doses of CNCP gained significant body weight (287.50 ± 13.69 gram) (Figure 3). Physical appearance of eye colour, the changes after feeding the rats with CNCP (LD) and CNBP (HD) at 45 days, the eye colour of those animals treated as well as those animals fed with glibenclamide were found to be completely normal when compared to the untreated diabetic rats who exhibited white eyes syndrome after 45 days. Their lenses also showed obvious lesions of pigmentary degeneration. Besides that, the untreated diabetic rats were detected to have thin and rough fur that was followed by obvious fur loss.

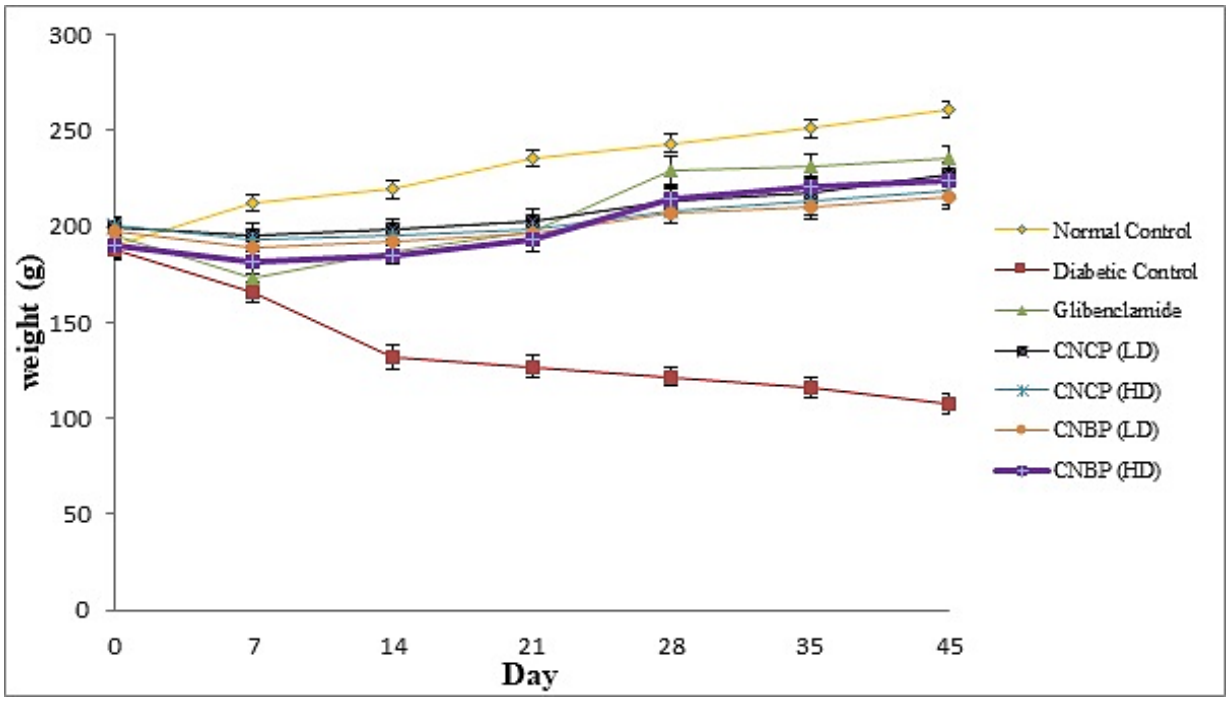

FIGURE 3 - Body weight changes of STZ-NA-induced diabetic and control rats for 45 days. All values are recorded as Mean ± SEM (n=6).

Measurement of insulin

Figure 4 illustrates the effects of CNCP and CNBP on insulin serum level of STZ-NA diabetic and normal rats. Serum insulin readings in the untreated control group significantly declined when compared to the healthy control group after 45 days' treatment (Figure 4). The treated rats with CNCP (LD) and CNBP (HD) fed groups showed high increase of the serum insulin level when compared to the untreated control group. In addition, the highest increase of the serum insulin belongs to the CNCP (LD, 28.98 ± 1.52) fed groups when compared to the untreated control group (6.56 ± 1.31). The findings suggested that there was an observation of improvements in glycemic control by CNCP (LD) and CNBP (HD) in the diabetic rats.

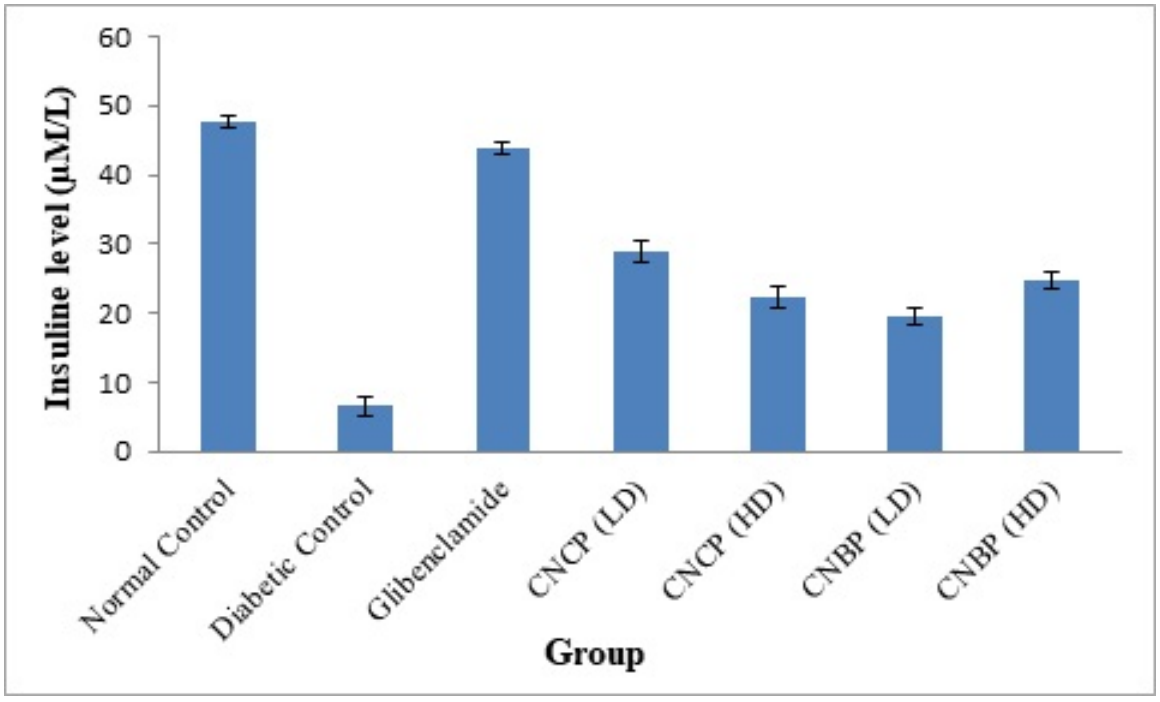

FIGURE 4 - Effects of CNCP and CNBP on serum insulin level of STZ-NA diabetic rats in comparison with untreated control rats after 45 days treatment. Data are presented as means ± SEM (n = 6). Significant difference compared to untreated control ($^{*}p < 0.05$).

Histological evaluation

Histological investigations of liver

As depicted in Figure 5, the tissue sections of the liver were stained with hematoxylin and eosin. Picture A shows the healthy control group rats showed normal hepatic architecture with normal hepatocyte morphology, organized hepatic cell (Hc) cords, and portal vein (Pv) with sinusoidal cords (S). Picture B shows that the untreated control group had manifested severe pathological changes, such as disordered hepatic cords, focal necrosis, congestion in the portal vein, infiltration of lymphocytes, increase of Kupffer cells (Kc), and also dilated sinusoids (S). Picture C shows the glibenclamide in the reference group showed positive effect on diabetic rats' pathological changes. Picture D shows that in the CNCP (LD) treated group, the hepatic architecture of liver was similar to that of the normal hepatic architecture and was characterized by normal central vein and hepatocytes with no fatty changes and containing mild RBC infiltration. Picture E and F

clearly illustrated CNCP (HD) and CNBP (LD) caused sinusoid remained dilated with RBC and central vein in an orderly manner in the liver of the diabetic rats. Finally, picture G demonstrates that CNBP (HD) caused a small amount of inflammatory cell infiltration on diabetic rat liver.

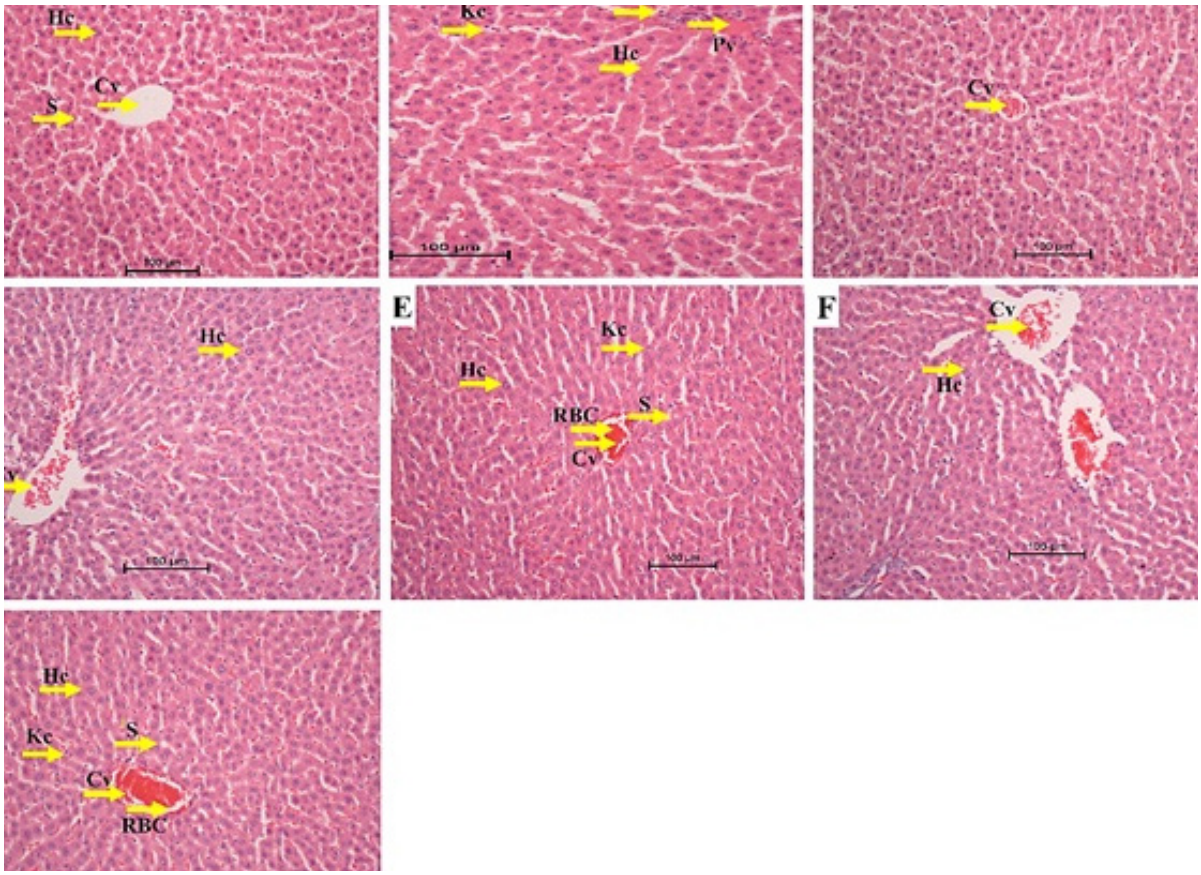

FIGURE 5 - H & E staining of liver tissues of SD rats (n=6). (A) Normal, (B) Diabetic, (C) Reference control (Glibenclamide), (D) CNCP, (E) CNCP, (F) CNBP and (G) CNBP. Normal hepatic architecture. B shows that untreated control resulted in severe pathological changes, such as increase in Kuppfer cells (Kc), and dilation sinusoids (S). D shows highest effect obtained by CNCP treatment on the liver of diabetic rat. Hepatic architecture was similar to the normal architecture (C). Scale bar: 100 µm. Abbreviations: Hepatic cell (Hc), Portal vein (Pv), Central vein (Cv).

Histological investigations of kidney

Figure 6 indicates rat kidney sections stained with haematoxylin and eosin. As shown in picture A, healthy control rat kidneys showed normal glomerulus, which was surrounded by Bowman's capsule, distal convoluted tubules and proximal with no inflammatory changes. In addition, normal capillaries (CP), and normal podocytes (Pc) were observed in kidney sections of the control group. On the contrary, picture B depicts that kidney sections of the untreated control rats contained degenerated glomeruli which was infiltrated by inflammatory cells and basement membrane thickness. The proximal convoluted tubule showed edematous changes with deposition of mucopolysaccharide and hyaline substances. Furthermore, it contained severe pathological damages including mesangial expansion and glomerular hypertrophy, which could cause loading of the Bowman's capsule space and adhesion of capillaries to the wall. Picture C shows that glibenclamide (reference group) showed positive effect on diabetic rats' pathological changes. As shown in picture D and G, CNCP (LD)

and CNBP (HD) showed no clear histopathological abnormalities or decreased expansion of glomerular and mesangial matrix in the renal sections. Both pictures E and F show the effect of CNCP (HD) and CNBP (LD) on diabetic rat's kidney, which verified the moderate changes of the kidney tissue.

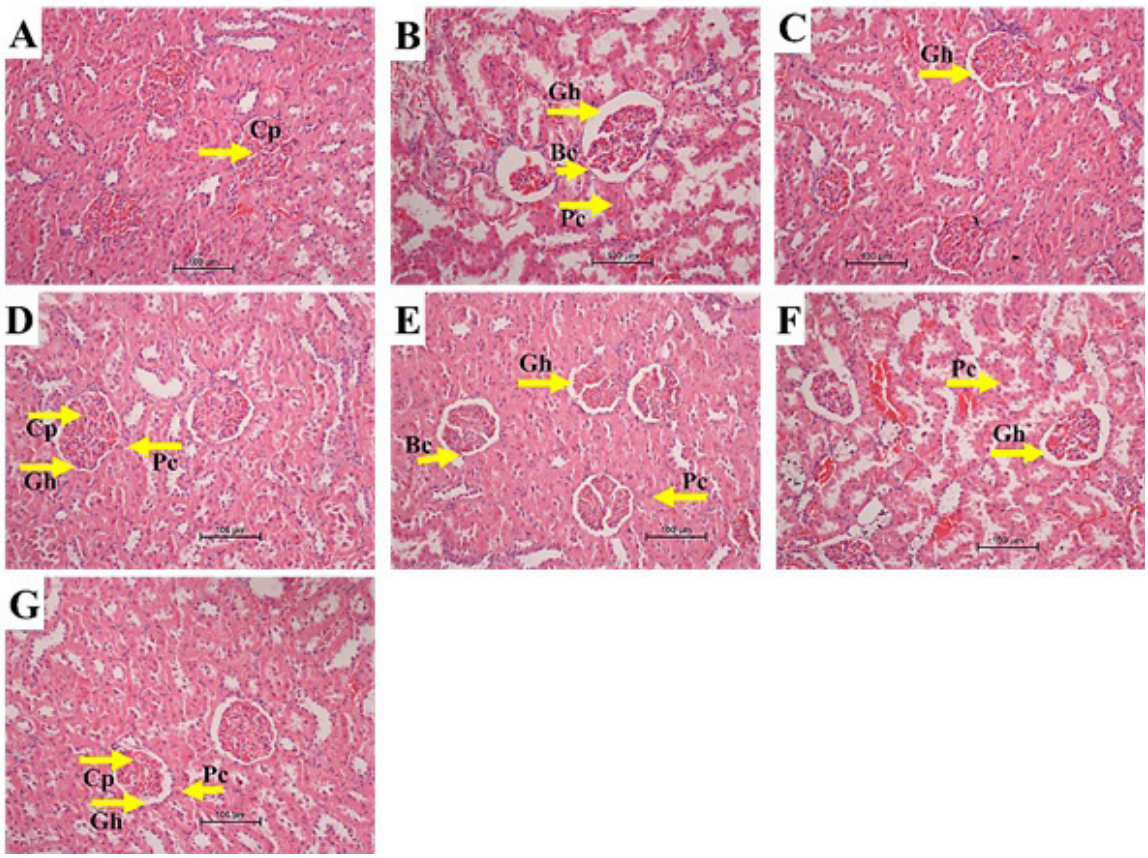

FIGURE 6 - H & E staining of kidney tissues of SD rats (n=6). A) Normal (B) Diabetic (C) Reference control (Glibenclamide), (D) CNCP and (E) CNCP, (F) CNBP and (G) CNBP. In diabetic rats (B), there is a significant damage to the glomeruli (hypertrophy, hypercellularity, tubules dilatation and atrophy) compared to the healthy control(A). Treatment of CNCP (10 mg/ml) and CNBP (20 mg/ml) attenuated the kidney alteration (D and G) in diabetic rats, which are comparable with the reference control (C) on the STZ-NA-induced pathological changes. Scale bar: 100 µm. Abbreviations: Bowman's capsule (Bc), Podocytes (Pc), Capillaries (CP), Glomerular hypertrophy (Gh).

Staining results of the rat's pancreas sections with hematoxylin and eosin are shown in Figure 7. In picture A, the healthy control group's pancreatic section shows normal islets of Langerhans, normal pancreatic structure, and normal tissues. Picture B shows disorganization of structure of the endocrine and exocrine cells with some damages, necrotic pancreatic acini and islet shrinkage. As shown in picture C, the reference control group exhibits the most interesting aspect of examined pancreatic sections, which shows normal islets of Langerhans. In picture D and G, effect of CNCP (LD) and CNBP (HD) on diabetic rat's liver demonstrated that these factors could much better promote cell survival and provide a much healthier structure. Effects of the CNCP (HD) and CNBP (LD) on the diabetic rat pancreas (picture E and F) display moderate restoration of the pancreatic cells.

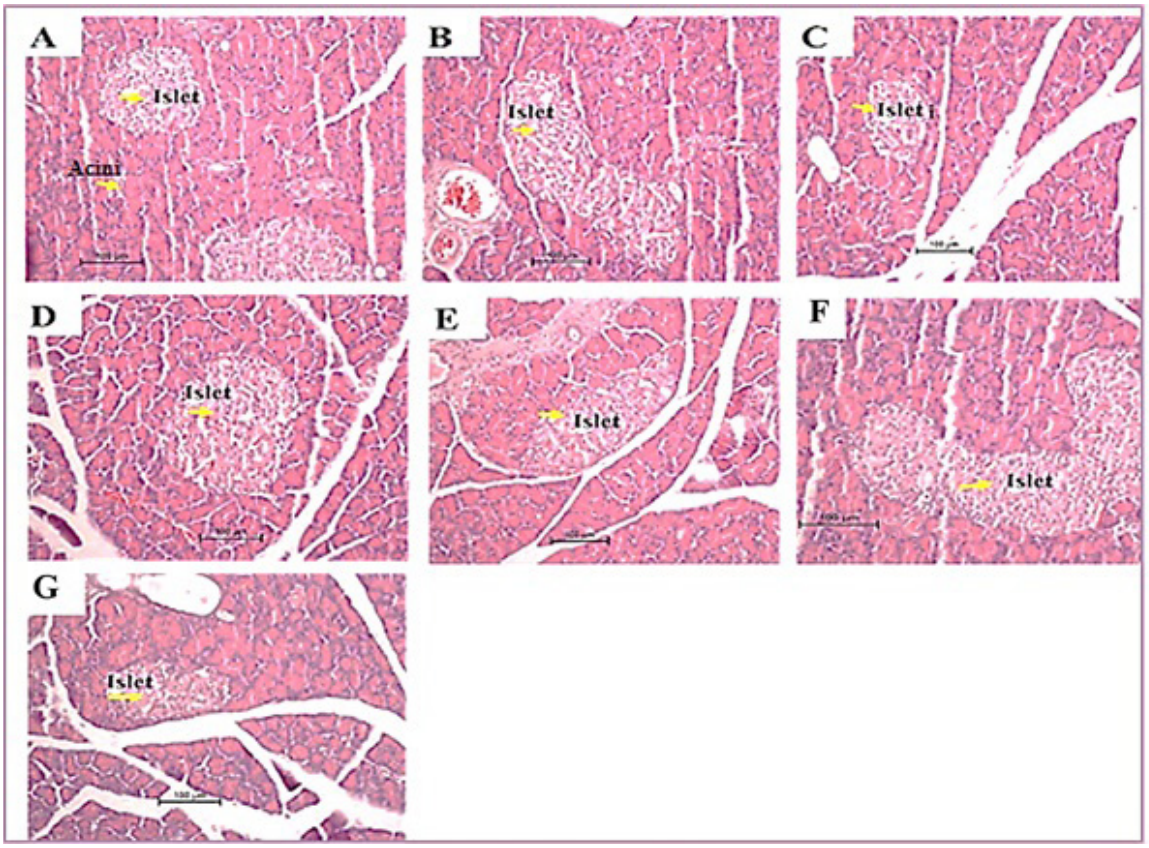

FIGURE 7 - H & E staining of pancreas tissues of SD rats (n=6). A) Normal, (B) Diabetic, (C) Reference control (Glibenclamide), (D) CNCP and (E) CNCP, (F) CNBP (10 mg/kg) and (G) CNBP (20 mg/kg). In picture (A), healthy controlpancreatic section showed normal islets of Langerhans. B shows a disorganisation of the pancreatic structure. C shows normal islets of Langerhans. D: the effect of CNCP (10 mg/kg) on diabetic rat's pancreas demonstrates that these factors better promoted the cells and provides a more healthy structure and shows a prominent hyperplastic islet and improved islet morphology. Scale bar: 100 µm.

DISCUSSIONS

In the current pilot study, CNCP at lower dose (LD) showed highest activity to reduce hyperglycaemia after six weeks of treatment in comparison with CNCP (HD) and CNBP (HD and LD). Moreover, both compounds showed beneficial pharmacological effect on diabetic, liver functional tests and lipids profile.

Concerning normalized serum lipids profile, CNCP (LD) was shown to boost the levels of the enzymes markers (AST, ALT, and ALP) back to the normal value. This result suggests that CNCP (LD) could be beneficial compound in preventing hepatocellular damage and tissue necrosis via suppression of gluconeogenesis; while, the other compounds showed sufficient activity but at lower levels. Antioxidant properties in both Schiff base compounds might also help restore liver damages (Asadi-Samani *et al.*, 2015). Also, CNCP and CNBP (Saremi *et al.*, 2019) showed acceptable antioxidant activity, but CNCP with lower IC_{50} than CNBP was found to be more potent. Due to higher antioxidant activity of CNCP rather than CNBP, the difference between lowering enzyme activates between these compounds could be reasonable.

It is well known that hyperlipidemia is a typical feature during hyperglycemia in diabetes. As shown in the current study, total cholesterol and LDL cholesterol levels increased significantly in serum of the untreated control animals; whereas the level of HDL cholesterol was found to be decreased. In contrast, it was found that successive administration of CNCP (LD) could reduce total and LDL cholesterol levels and increase

HDL cholesterol, which could suggest that CNCP (LD) possessed noticeable hypolipidemic effect. During oxidative stress, ROS cause to oxidation unsaturated lipids existing in external layer of LDL or in lipid bilayer of bio membrane, leading to accumulating secondary products of free radical oxidation, namely, malondialdehyde (MDA) (Kumskova *et al*., 2014). Schiff bases with high antioxidant activity are able to decrease LDL level and reversely increase HDL in blood by suppressing free radicals (Mabuza *et al*., 2019, Torabi, Mohammadi, Shirvani, 2018, Sykuła *et al*., 2018). Hence, it can be suggested that hypolipidemic effect of CNCP (LD) could be associated with higher antioxidant activity when compared with CNBP (Kumskova *et al*., 2014).

It is suggested that both CNCP (LD) and CNBP (HD) could decrease the elevated blood glucose level in untreated control group and helped the glucose levels turned back to the normal range values, but CNCP (LD) was found to be more potent than CNBP (HD). As the matter of fact, it can be implied that antidiabetic effect of the novel Schiff base compounds might exhibit an oxidation state dependent effect on blood glucose levels; however, the chlorine substituted compound having higher antioxidant activity could be more active in lowering blood glucose levels. Hyperglycaemia in diabetes disease is regarded as the main symptom caused by lack of insulin and/or insulin resistance (Ke *et al*., 2009). It is anticipated that the both Schiff bases, especially, CNCP (LD) could decrease glucose levels in the blood maybe via increasing either regeneration of pancreatic islets or increasing insulin release in the STZ-NA-induced diabetic rats (Schuit *et al*., 2001; Mabuza *et al*., 2019).

In the histopathology study, the healthy control group showed several pathological changes and were listed in the results section. In the diabetic liver, unorganized hepatocytes, granular degeneration, micro-vesicular vacuolization and necrosis were the marked changes, which are, detected (Zhou *et al*., 2008). Efforts are made for finding out and trying to decipher the main molecular mechanisms, which are responsible for β-cell death in diabetes. It is suggested that apoptosis is likely as the main cause of such destruction (Thomas, Kay, 2000). In the current study, severity of hepatic injuries in the SD rats is reduced with treatment of CNCP (LD). It is demonstrated by the results that the pancreas tissues of the diabetic rats could reduce the amount of islets, degeneration of *β*-cells, hydropic degeneration, clumping of *β*-cells, pyknosis, and necrosis, which caused changes in cells morphology due to STZ-NA-induced partial damages in some *β*-cells which alignes with some other studies (Roat *et al*., 2014). Furthermore, islet cells might be restored by CNCP (LD), which means that treatment was capable to recover these degenerated cells. Unlike CNBP, the administration of increased individual dose of CNCP administered to diabetic animals showed a comprehensive reversible effect. This finding implied that CNCP (10 mg/kg) and CNBP (20 mg/kg) treated groups compared to the groups treated with the higher dose of CNCP (20 mg/kg) and CNBP (10 mg/kg) indicated better function on the cells. Diabetic nephropathy (DN) is one of those key complications connecting with diabetes and accompanied with expansion of mesangial cells, as hallmark of diabetic rats (Matsubara *et al*., 2006), accumulation of extracellular matrix protein, thickening of glomerular and tubular basement membranes, tubulointerstitial fibrosis, glomerulosclerosis, renal endothelial dysfunction, albuminuria, proteinuria, and also reduction in glomerular filtration rate (Balakumar *et al*., 2009). In the current study, the diabetic SD rats control group displayed acute swelling of cells, hydropic degeneration of tubules, widening of Bowman's space, glomerular atrophy, congestion of capillaries, and tubular necrosis. Drastic pathological changes were also observed in focal mesangial matrix expansion, proteinuria, and significant increase in albuminuria of diabetic animals compared to the healthy control group. CNCP (LD) could ameliorate meningeal expansion, proteinuria, and albuminuria, which confirmed that CNCP at 10 mg/kg in comparison with CNBP at both doses could be the best and more beneficial treatment dose for alleviating histological injuries. However, such outcomes still require further delineation to completely understand the underlying molecular mechanisms of two compounds which helps us to find the reasons behind more effectiveness of CNCP (10mg/kg) than the other dose and CNCB (LD and HD).

CONCLUSION

Although CNCP and CNBP at both doses showed some antidiabetic effect in STZ-NA-induced diabetic rat model, CNCP (LD) could possibly exert the highest anti-hyperglycaemic effect. CNCP (LD) was the most successful compound compared to CNCP (HD) and both doses of CNBP in decreasing insulin level and showed higher protective effect on liver, kidney, and pancreatic β-cells. These findings propose that CNCP, a chlorine substitute Schiff base was an excellent candidate for treating diabetic complications. However, bromine substitute of the same Schiff base showed acceptable antidiabetic effect. In summary, the study shows new Schiff base derivatives showed antidiabetic potential, which could be associated to their antioxidant activity in diabetic rats.

ACKNOWLEDGEMENTS

The authors would like to thank the University of Malaya for financial support IPPP grant number (PG074-2015B) and providing grant funding to conduct this study.

AUTHOR CONTRIBUTIONS

Acquisition of data: KS; analysis and interpretation of data: KS; drafting of manuscript: KS and SKR; ZSH: critical revision: KS, SKR, NA.

REFERENCES

Afzal HR, Khan NUH, Sultana K, Mobashar A, Lareb A, Khan A, et al. Schiff bases of pioglitazone provide better antidiabetic and potent antioxidant effect in a streptozotocin nicotinamide-induced diabetic rodent model. ACS Omega. 2021;6(6):4470-4479.

Al-Qadsy I, Saeed WS, Al-Odayni AB, Ahmed Saleh Al-Faqeeh L, Alghamdi AA, Farooqui M. Novel metformin-based schiff bases: synthesis, characterization, and antibacterial evaluation. Materials. 2020;13(3):514.

Anitha C, Sheela C, Tharmaraj P, Shanmugakala R. Studies on synthesis and spectral characterization of some transition metal complexes of azo-azomethine derivative of diaminomaleonitrile. Int J Inorg Chem. 2013(2013):Article ID 436275.

Asadi-Samani M, Kafash-Farkhad N, Azimi N, Fasihi A, Alinia-Ahandani E, Rafieian-Kopaei M. Medicinal plants with hepatoprotective activity in Iranian folk medicine. Asian Pac J Trop Biomed. 2015;5(2):146-157.

Balakumar P, Arora MK, Ganti SS, Reddy J, Singh M. Recent advances in pharmacotherapy for diabetic nephropathy: current perspectives and future directions. Pharmacol Res. 2009;60(1):24-32.

Bedia KK, Elçin O, Seda U, Fatma K, Nathaly S, Sevim R, et al. Synthesis and characterization of novel hydrazide–hydrazones and the study of their structure antituberculosis activity. Eur J Med Chem. 2006;41(11):1253-1261.

El-Hashash MA, Kadhim MA, Rizk SA. Facile synthesis, characterization of novel schiff bases and N-nucleosides bearing quinazoline moiety and evaluation of their antimicrobial effects. J Appl Chem. 2015;4:1716-1724.

Gupta SK. Topical delivery system for antiaging and skin whitening agents. Google Patents. 2010.

Kakkar R, Kalra J, Mantha SV, Prasad K. Lipid peroxidation and activity of antioxidant enzymes in diabetic rats. Mol Cell Biochem. 1995;151(2):113-119.

Ke YD, Delerue F, Gladbach A, Götz J, Ittner LM. Experimental diabetes mellitus exacerbates tau pathology in a transgenic mouse model of alzheimer's disease. Plos One. 2009;4:E7917.

Kim SJ. Herbal Chrysanthemi Flos, oxidative damage and protection against diabetic complications. Diabetes: Oxidative Stress and Dietary Antioxidants. Elsevier. 2014.

Küçükgüzel ŞG, Küçükgüzel İ, Oral B, Sezen S, Rollas S. Detection of nimesulide metabolites in rat plasma and hepatic subcellular fractions by Hplc-Uv/Dad and Lc-Ms/Ms studies. Eur J Drug Metab Pharmacokinet. 2005;30(1-2):127-134.

Kumar M, Padmini T, Ponnuvel K. Synthesis, characterization and antioxidant activities of schiff bases are of cholesterol. J Saudi Chem Soc. 2017;21:S322-S328.

Kumskova EM, Antonova OA, Balashov SA, Tikhaze AK, Melkumyants AM, Lankin, VZ. Malonyldialdehyde and glyoxal act differently on low-density lipoproteins and endotheliocytes. Mol Cell Biochem. 2014;396(1-2):79-85.

Lenzen, S. Chemistry and biology of reactive species with special reference to the antioxidative defence status in pancreatic B-cells. Biochim Biophys Acta Gen Subj. 2017;1861(8):1929-1942.

Lin X, Liu M. Bromophenols from marine algae with potential anti-diabetic activities. J Ocean Univ China. 2017;11:533-538.

This is an open-access article distributed under the terms of the Creative Commons Attribution License.

Lobo V, Patil A, Phatak A, Chandra N. Free radicals, antioxidants and functional foods: impact on human health. Pharmacogn Rev. 2010;4(8):118-126.

Mabuza LP, Gamede MW, Maikoo S, Booysen IN, Ngubane PS, Khathi A. Cardioprotective effects of a ruthenium (II) schiff base complex in diet-induced prediabetic rats. Diabetes Metab Syndr Obes. 2019;12:217-223.

Mahmoud M, Zaitone S, Ammar A, Sallam S. Synthesis, structure and antidiabetic activity of chromium (III) complexes of metformin schiff bases. J Mol Struct. 2016;1108:60-70.

Matsubara T, Abe H, Arai H, Nagai K, Mima A, Kanamori H, et al. Expression of smad1 is directly associated with mesangial matrix expansion in rat diabetic nephropathy. Lab Invest. 2006;86(4):357-368.

Masiello P, Broca C, Gross R, Roye M, Manteghetti M, Hillaire-Buys D, Novelli M, Ribes G. Experimental NIDDM: development of a new model in adult rats administered streptozotocin and nicotinamide. Diabetes. 1998;47:224-229.

Ndagi U, Mhlongo N, Soliman ME. Metal complexes in cancer therapy–an update from drug design perspective. Drug Des Devel Ther. 2017;11:599–616.

Niizato T, Shiotani M, Shoji Y. Composition for treatment of diabetes and treatment of diabetes. Google Patents. 2002.

Noshahr ZS, Salmani H, Khajavi Rad A, Sahebkar A. Animal models of diabetes associated renal injury. J Diabetes Res. 2020: 9416419.

Roat R, Rao V, Doliba NM, Matschinsky FM, Tobias JW, Garcia E, et al. Alterations of pancreatic islet structure, metabolism and gene expression in diet-induced obese C57bl/6j mice. Plos One. 2014;9:E86815.

Rollas S, Gulerman N, Erdeniz H. Synthesis and antimicrobial activity of some new hydrazones of 4-fluorobenzoic acid hydrazide and 3-Acetyl-2, 5-Disubstituted-1, 3, 4-Oxadiazolines. Farmaco. 2002;57(2):171-174.

Sahiba N, Sethiya A, Soni J, Agarwal DK, Agarwal S. Saturated five-membered thiazolidines and their derivatives: from synthesis to biological applications. Top Curr Chem. 2020;378(2):1-90.

Saremi K, Rad SK, Khalilzadeh M, Hussaini J, Majid NA. In vivo acute toxicity and anti-gastric evaluation of a novel dichloro schiff base: Bax and Hsp70 alteration. Acta Biochim Biophys Sin (Shanghai). 2020;52(1):26-37.

Saremi K, Rad SK, Tayeby F, Abdulla MA, Karimian H, Majid NA. Gastroprotective activity of a novel schiff base derived dibromo substituted compound against ethanol-induced acute gastric lesions in rats. BMC Pharmacol Toxicol. 2019;20(1):13.

Schuit FC, Huypens P, Heimberg H, Pipeleers DG. Glucose sensing in pancreatic B-cells: A model for the study of other glucose-regulated cells in gut, pancreas, and hypothalamus. Diabetes. 2001;50(1):1-11.

Shima K, Zhu M, Kuwajima M. A role of nicotinamide-induced increase in pancreatic B-cell mass on blood glucose control after discontinuation of the treatment in partially pancreatectomized oletf rats. J Diabetes Res. 1998;41(1):1-8.

Shukla SN, Gaur P, Jhariya S, Chaurasia B, Vaidya P, Azam M. Biochemical relevance of Cr (Iii) complexes of isoniazid: synthesis, characterization, Dft, antibacterial screening, antioxidant activity and glucose-lowering effect in stz-induced diabetic rats. J Coord Chem. 2019;72(4):664-689.

Sirajuddin M, Ali S, Haider A, Shah NA, Shah A, Khan MR. Synthesis, characterization, biological screenings and interaction with calf thymus Dna as well as electrochemical studies of adducts formed by azomethine [2-((3, 5-Dimethylphenylimino) Methyl) Phenol] and organotin (Iv) chlorides. Polyhedron. 2012;40(1):19-31.

Sykuła A, Cheshchevik VT, Cheshchevik NG, Dzeikala A, Łodyga-Chruścińska E. In vitrostudy of hesperetin schiff bases antioxidant activity on rat liver mitochondria. Biotechnol Food Sci. 2018;82(2):151-159.

Thomas HE, Kay TW. Beta cell destruction in the development of autoimmune diabetes in the Non-Obese Diabetic (Nod) mouse. Diabetes Metab J. 2000;16(4):251-261.

Torabi S, Mohammadi M, Shirvani M. Antidiabetic, antioxidant, antibacterial, and antifungal activities of vanadyl schiff base complexes. Trends Pharmacol Sci. 2018;4:87-94.

Vančo J, Marek J, Trávníček Z, Račanská E, Muselík J, Švajlenová OG. Synthesis, structural characterization, antiradical and antidiabetic activities of copper (Ii) and zinc (Ii) schiff base complexes derived from salicylaldehyde and B-alanine. J Inorg Biochem. 2008;102(4):595-605.

Yaul A, Pethe G, Deshmukh R, Aswar A. Vanadium complexes with quadridentate schiff bases. J Therm Anal Calorim. 2013;113:745-752.

Zhao X, Wu H, Guo B, Dong R, Qiu Y, Ma PX. Antibacterial anti-oxidant electroactive injectable hydrogel as self-healing wound dressing with hemostasis and adhesiveness for cutaneous wound healing. Biomaterials. 2017;122:34-47.

Zhou JY, Zhou SW, Zhang KB, Tang JL, Guang LX, Ying Y, et al. Chronic effects of berberine on blood, liver glucolipid metabolism and liver ppars expression in diabetic hyperlipidemic rats. Biol Pharm Bull. 2008;31(6):1169-1176.

Received for publication on 09th March 2021
Accepted for publication on 20th April 2022